










Piezo-, photo- and piezophotocatalytic activity of electrospun fibrous PVDF/CTAB membrane

Alina Rabadanova ^a , Magomed Abdurakhmanov ^a , Rashid Gulakhmedov ^a ,
Abdulatip Shuaibov ^a , Daud Selimov ^a , Dinara Sobola ^{a,b} ,
Klára Částková ^c , Shikhgasan Ramazanov ^d , Farid Orudzhev ^{a,d,e} * 

a: Smart Materials laboratory, Dagestan State University, Makhachkala 367015, Russia

b: Department of Physics, Faculty of Electrical Engineering and Communication, Brno University of Technology, Brno 61600, Czech Republic

c: CEITEC BUT – Brno University of Technology, Brno 61200, Czech Republic

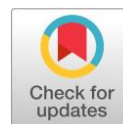
d: Amirkhanov Institute of Physics of Dagestan Federal Research Center, Russian Academy of Sciences, Makhachkala 367003, Russia

e: REC Smart Materials and Biomedical Applications, Immanuel Kant Baltic Federal University, Kaliningrad 236041, Russia

* Corresponding author: farid-stkha@mail.ru

This paper belongs to a Regular Issue.

© 2022, the Authors. This article is published in open access under the terms and conditions of the Creative Commons Attribution (CC BY) license (<http://creativecommons.org/licenses/by/4.0/>).



Abstract

A composite material based on polyvinylidene fluoride (PVDF) nanofibers modified with cetyltrimethylammonium bromide (CTAB) was synthesized by coaxial electrospinning. The morphology and structure of the material were studied by SEM, FTIR spectroscopy, X-ray diffraction analysis, XPS, and the piezo-, photo- and piezophotocatalytic activity during the decomposition of the organic dye Methylene blue (MB) was studied. It was shown that the addition of CTAB promotes additional polarization of the PVDF structure due to the ion-dipole interaction. It was shown for the first time that the addition of CTAB promotes the photosensitivity of the wide-gap dielectric polymer PVDF (the band gap is more than 6 eV). It was demonstrated that the photocatalytic decomposition efficiency is 91% in 60 minutes. The material exhibits piezocatalytic activity – 73% in 60 minutes. The experiments on trapping active oxidizing forms established that OH hydroxyl radicals play the main role in the photocatalytic process.

Keywords

PVDF
photocatalysis
piezocatalysis
piezophotocatalysis
nanofibers
coaxial electrospinning
CTAB
methylene blue

Received: 18.10.22

Revised: 07.11.22

Accepted: 10.11.22

Available online: 17.11.22

1. Introduction

Water pollution caused by persistent organic dyes is a serious environmental problem. Various effective methods have been developed to eliminate pollution, such as absorption, electrochemical treatment, photocatalysis, piezocatalysis, piezophotocatalysis [1]. However, inappropriate band gap structure, low mobility rate, fast recombination of the generated charge carriers often limit the photocatalytic applications [2]. Recently, the internal electric field of piezoelectric materials that can be used to overcome the above limitations in the photocatalytic process has generated a lot of interest [3]. The piezoelectric effect is used to enhance photocatalysis by an internal electric field, which promotes the separation and migration of photogenerated electron-hole pairs, thereby realizing higher piezophotocatalytic efficiency for the simultaneous use of these two types of natural energy. Compared to the relatively mature research on

photocatalysis, piezocatalysis is seen as a new strategy for tackling environmental pollution and energy shortages [4]. So far, the research on piezocatalytic applications is still in its infancy. However, it is already clear from the available studies that the wide spread practical application of heterogeneous photo-, piezo- and piezophotocatalysts in the suspension mode is difficult due to their uneven dispersion and the difficulty of extracting and reusing the catalysts. The solution to these problems can be the immobilization of the catalyst on a polymer matrix. A recent review [5] summarized significant progress in the preparation of various photocatalytic materials based on hybrid polymers. In recent years, polymer composites based on PVDF and semiconductor nanoparticles, the so-called heterophase doping, have been intensively studied for the purposes of piezocatalysis and piezophotocatalysis [6–9]. Moreover, poly(vinylidene fluoride) (PVDF) can crystallize into at least four polymorphs (α , β , γ and δ), which leads to different ferroelectric properties.

Compared to the α -phase, the polar β - and γ -phases have attracted a lot of attention due to their unique physical properties and potential applications [10]. For example, the polar phases, β and γ , cause pyroelectricity, piezoelectricity, and ferroelectricity. Meanwhile, the γ -phase increases transparency, which makes it suitable for optical devices. To obtain the maximum content of the β phase in PVDF membranes, various approaches are used, among which the most effective are the choice of a synthesis method and the addition of various fillers [11]. One of the most effective methods for the synthesis of PVDF with the maximum content of the β phase is considered to be electrospinning, in which high voltages contribute to the repolarization of the structure due to the alignment of electric dipoles. A recent review [12] summarized the generalized approaches to the fabrication of hybrid piezoelectric materials based on PVDF and its copolymer, poly-(vinylidene fluoride)-trifluoroethylene PVDF-TrFE with fillers of inorganic and metal nanoparticles, conductive rGO nanosheets and others to improve the piezoelectric characteristics of composites and their practical application as mechanical energy converters. However, for photocatalytic applications, composite polymer-inorganic structures have their own specific requirements [13]. In most studies, composites are synthesized by phase inversion, in which most of the nanoparticles are in the bulk of the polymer membrane, which limits the access of light and solution to the surface of the nanoparticles. Proceeding from this, the actual task of materials science is to find a method for homophase doping of PVDF to give it new functional properties. The previous reports have demonstrated that the addition of a low concentration of the cationic surfactant cetyltrimethylammonium bromide (CTAB) can effectively induce a pure γ -phase by introducing a strong ion-dipole interaction between the CTAB and PVDF dipoles [14, 15]. In [16] the authors reported the piezocatalytic activity of pure PVDF and its copolymer with hexafluoropropylene (HFP) to produce hydrogen under ultrasonic irradiation.

In this study, we synthesized a composite PVDF/CTAB nanofiber membrane by electrospinning. It was shown that doping with CTAB leads to photosensitization of the polymer. It was also shown for the first time that a PVDF polymer membrane exhibits high piezocatalytic and photocatalytic activity towards the decomposition of methylene blue.

It was demonstrated for the first time that irradiation with UV-visible light leads to the suppression of piezocatalytic properties during piezophotocatalysis.

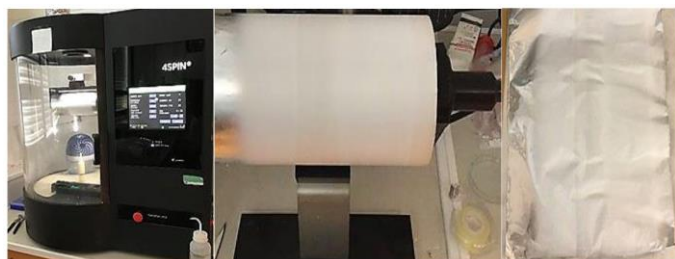


Figure 1 Contipro 4SPIN LAB electrospinning device and the image of the resulting sample.

2. Methodology

2.1. Synthesis of PVDF/CTAB nanofibers

For electrospinning, PVDF with a molecular weight of 275,000 g mol⁻¹ (Sigma Aldrich, St. Louis, MO, USA) was used. Dimethyl sulfoxide (DMSO, Sigma Aldrich, St. Louis, MO, USA) and acetone (Ac, Sigma Aldrich, St. Louis, MO, USA) were used as solvents. CTAB (Sigma Aldrich, St. Louis, MO, USA) was added as a surfactant.

PVDF with a concentration of 20 wt.% was dissolved in the binary solvent dimethyl sulfoxide/acetone in a volume ratio of 7/3 at 50 °C for 24 h until a visually homogeneous solution was formed. A PVDF/CTAB solution was prepared by modification of the neat PVDF solution with 1 wt.% CTAB (by weight of solution). PVDF nanofibers were produced by coaxial electrospinning on a Contipro 4SPIN LAB facility (Contipro as, Dolni Dobrouc, Czech Republic). A coaxial setup included two syringes to feed PVDF and PVDF/CTAB solutions independently to a coaxial tip consisting of two concentric needles. The interior needle had an inner diameter of 0.514 mm and was set 0.5 mm longer than the exterior one at the end of the tip. The outer needle had an inner diameter of 1.372 mm. The coaxial electrospinning was performed with feeding rates of 9 μ l/min at a constant voltage of 50 kV and a collector rotation speed of 2000 rpm. The distance between the tip of the needle and the collector (a rotating metal drum covered with aluminium foil) was 20 cm. The processing time was 30 minutes. Visually, the process is shown in Figure 1.

2.2. Characterization and analysis of nanofibers

The morphology of the samples was studied using a scanning electron microscope (SEM) LYRA3 (Tescan, Brno, Czech Republic). The samples were coated with a 15 nm carbon layer using a Leica EM ACE600 coater (Leica Microsystems, Wetzlar, Germany). Mean fiber diameters were calculated from the SEM images using ImageJ software.

The XRD analysis was performed with an X-ray powder diffractometer Rigaku SmartLab 3 kW (Rigaku Corporation, Tokyo, Japan) in the Bragg-Brentano configuration. Diffraction patterns were obtained between 10 ° and 50 ° (2 θ) with Cu K α radiation.

XPS spectra were recorded on an AXIS SupraTM X-ray photoelectron spectrometer (Kratos Analytical Ltd., Manchester, UK) with an emission current of about 15 mA. The spectra were adjusted using CasaXPS v.2.3.23 program.

The measurement of FT-IR spectroscopy was carried out in transmission mode using a Bruker spectrometer (BillERICA, Massachusetts, USA) with a resolution of 1 cm⁻¹ and 512 iterations.

2.3. Piezophotocatalytic experiment

The piezocatalytic/piezophotocatalytic decomposition test was carried out using UV-visible irradiation. A 250 W high-pressure mercury lamp (Philips) was used as a source of UV-visible light. The distance from the light source to the

reactor was 10 cm. Piezophotocatalytic decomposition was carried out in an ultrasonic (US) bath with a power of 250 W at a frequency of 18 kHz. To eliminate the effect of temperature on the decomposition efficiency, the reactor was kept at a constant temperature of 26 °C. Before testing, a film (3x1 cm², thickness 25 μm, weight 0.7 mg) was immersed in a beaker with a solution of methylene blue (MB) (1 mg L⁻¹, 20 mL) and kept in a dark place for 1 h to establish the adsorption-desorption balance. During the test, 3 ml of the sample solution was taken every 15 min and analyzed using a UV-visible spectrometer. The dye concentration was measured from the maximum absorption peak λ = 663 nm. The percentage of degradation was indicated as C/C₀ (C and C₀ are the measured and initial concentrations of the dye solution, respectively).

3. Results and Discussions

The morphology of the samples was characterized using a scanning electron microscope (SEM). Figure 2 shows the SEM images of the films of PVDF/CTAB nanocomposite fibers obtained by electrospinning. To determine the particle size distribution, the SEM image was examined using ImageJ.

It can be seen that the surface and structure are smooth, uniform, without visible defects. The PVDF/CTAB fibers are formed as elongated nanofibers with different diameters. From the distribution histogram obtained using ImageJ program, it can be seen that the average diameter of the nanofibers is about 450 nm.

To determine the phase composition, the samples were characterized using FTIR spectroscopy and XRD. The data are presented in Figure 3. The XRD measurements of the PVDF/CTAB nanofibers show that the predominant phase is the β-phase. The peaks at 20.6 ° (110/200) and 36.6 ° (101) testify to this [17, 18] (Figure 2a). The diffraction bands of the monoclinic α phase peaks are located at 18.4 ° (020) and 41.1 ° (111). Since the diffraction bands of the γ and α phases overlap and it is not possible to accurately determine the phase distribution, FTIR analysis was used to quantify the phase distribution in PVDF.

From the FTIR spectra, the relative abundance of all three α-, β- and γ-phases in the samples were calculated. First, the fraction of the electroactive phase (F_{EA}) was calculated, according to equation 1:

$$F_{EA} = \frac{I_{EA}}{\left(\frac{K_{840}}{K_{763}}\right) I_{763} + I_{EA}} \cdot 100\% \quad (1)$$

where I_{EA} and I_{763} are the absorbances at 840 and 763 cm⁻¹, respectively; K_{840} and K_{763} are the absorption coefficients at the respective wave numbers, whose values are 7.7·10⁴ and 6.1·10⁴ cm² mol⁻¹, respectively. Then, using equations 2 and 3, the distribution of β- and γ-phases in the electroactive phase was calculated:

$$F(\beta) = F_{EA} \frac{\Delta H_{\beta'}}{\Delta H_{\beta'} + \Delta H_{\gamma'}} \cdot 100\% \quad (2)$$

and

$$F(\gamma) = F_{EA} \frac{\Delta H_{\gamma'}}{\Delta H_{\beta'} + \Delta H_{\gamma'}} \cdot 100\%, \quad (3)$$

where $\Delta H_{\beta'}$ and $\Delta H_{\gamma'}$ are the height differences (absorbance differences) between the peak around at 1275 cm⁻¹ and the nearest valley around at 1260 cm⁻¹, and the peak around at 1234 cm⁻¹ and the nearest valley around at 1225 cm⁻¹, respectively [18].

The calculations showed that in pure PVDF the fraction of the α phase was 9.74%, the fraction of the γ phase was 4.71%, and the fraction of the β phase was 85.55%, respectively. After the modification of CTAB, the proportion of the β-phase increased to 90.34%, the proportion of the α-phase was 9.51%, and the proportion of the γ-phase was 0.15%. The effect of CTAB addition on the formation of pure PVDF γ-phase due to the ion-dipole interaction was previously reported for membranes prepared by thermally induced phase inversion (TIPS). At the same time, it was reported that in the presence of CTAB, the charges in CTAB molecules attract the PVDF chains due to ion-dipole interactions, and the PVDF chains tend to form a trans conformation that is favorable for the nucleation of the γ-phase, which leads to the suppression of the growth rate of the α-phase. However, our results show that the addition of CTAB leads to suppression of the growth of the γ-phase and an increase in the proportion of the β phase. This discrepancy is apparently explained by the contribution of electric polarization during electrospinning.

The chemical state of the surface was examined using XPS. The wide spectrum (see Figure 4a) shows peaks in the main levels of carbon (C1s), fluorine (F1s) and oxygen (O1s). The F1s ground level spectra can be well decomposed into two peak components associated with CF (686.5 eV) and CF₂ (687.4 eV), respectively [19].

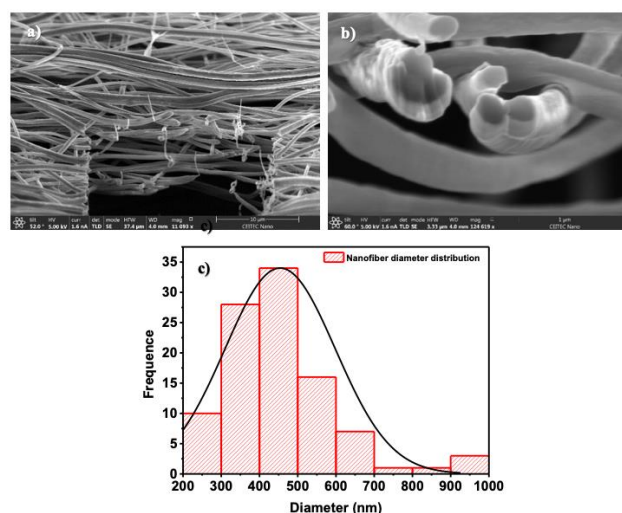


Figure 2 SEM images of PVDF/CTAB nanofibers at various magnifications (a, b) and the histogram of the distribution of nanofibers by diameter (c).

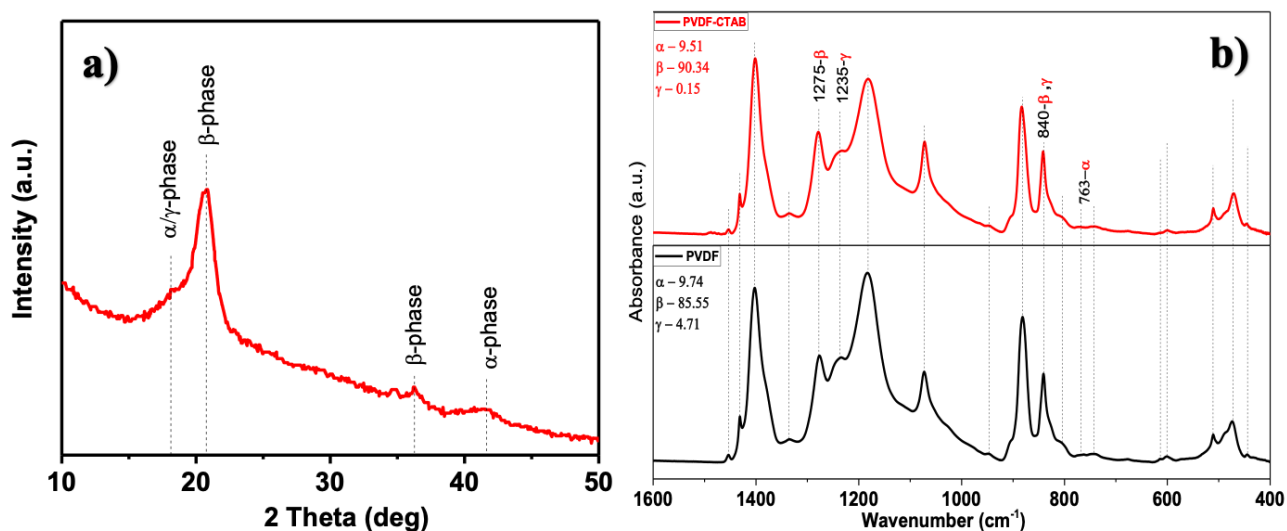


Figure 3 X-ray diffraction analysis of PVDF/CTAB nanofibers (a); IR Fourier spectrum of PVDF/CTAB nanofibers and pure PVDF (b).

These components can be attributed to the presence of covalent and semi-ionic fluorinated bonds. The previous work showed that pure PVDF has a high content of semi-ionic bonds [20, 21]. As is known, semi-ionic bonds are more oriented than covalent bonds, and a decrease in the proportion of semi-ionic bonds may indicate a decrease in the concentration of the more oriented β -phase. This result confirms the conclusions drawn from the FTIR spectra, where it was shown that the addition of CTAB leads to a change in the proportion of the β -phase by more than 5%. The changes in the concentration suggest that CTAB molecules bind to the PVDF structure and change the orientation of the polymer chain, rather than simply being located between individual fibers.

The XPS spectra of C1s (Figure 4c) show the presence of the standard bands expected for PVDF [22]. Deconvolution of the C1s spectrum identifies 6 peaks: C-C/C-H, CH_2 , C-O, FC-OH, CF_2 and CF_3 , among which the CH_2 peak is the most prominent. Deconvolution of the O1s peaks shows that the samples prepared with CTAB are enriched in oxygen-containing functional groups (Figure 4d), associated with residual oxygen from solvents and possible oxidative processes during the synthesis in open air.

Figure 5 shows the results of catalytic experiments in the decomposition of MS using a PVDF/CTAB membrane as a catalyst.

Two blank experiments were carried out in order to elucidate the contribution of MB self-decomposition under direct light (photolysis) and ultrasonic treatment (sonolysis). Blank experiments showed that MB degraded under the action of US treatment and UV-visible light, while the degree of degradation was 51.3% and 62.0% after 60 minutes.

The results of the piezocatalytic experiment, where the degree of dye decomposition was 73.0%, clearly indicate the generation of a piezopotential. When a sample is deformed by an external force from ultrasonic treatment, a polarization phenomenon occurs inside it, which generates positive and negative charges present on two

relative surfaces. Thus, an effective conversion of the external force into electrical energy occurs and a polarization electric field is generated, which contributes to the occurrence of redox chemical reactions, leading to the generation of highly active oxygen species, which oxidize the MB.

It can also be seen that the sample exhibits high photocatalytic activity – 93% of the dye decomposed in 60 minutes. The presence of PC activity under UV-visible irradiation in a polymer material whose band gap (BG), according to the literature data, is more than 6 eV, is an unexpected result and requires a deeper study of the electronic structure of the material. For example, in [23] using ultraviolet photoelectron and inverse photoemission spectroscopy, it was demonstrated that a change in the polarization state from positive to negative in the P(VDF-TrFE) ferroelectric caused a distinct shift of the valence band towards the Fermi level by 2.1 eV and the conduction band by 0.4 eV, as a result of which the BG decreased by 2.5 eV. It is likely that the addition of CTAB and the electrical polarization of the material during electrospinning facilitate the rearrangement of the electronic structure of PVDF, leading to a narrowing of the BG.

It is well known that photocatalytically active piezoelectric materials are widely used for photocatalytic wastewater treatment from organic pollutants, due to the because they are able to generate more free radicals with stronger oxidizing properties with the synergy of mechanical force and light [24].

Taking this into account, we studied the piezophotocatalytic oxidation of MB under the simultaneous action of ultrasonic and UV-visible irradiation.

The degree of MB decomposition in this case was 91%, which practically corresponds to the photocatalytic activity. This may probably indicate that, upon photoexcitation of PVDF/CTAB, a large number of photogenerated charge carriers suppress the piezoelectric properties.

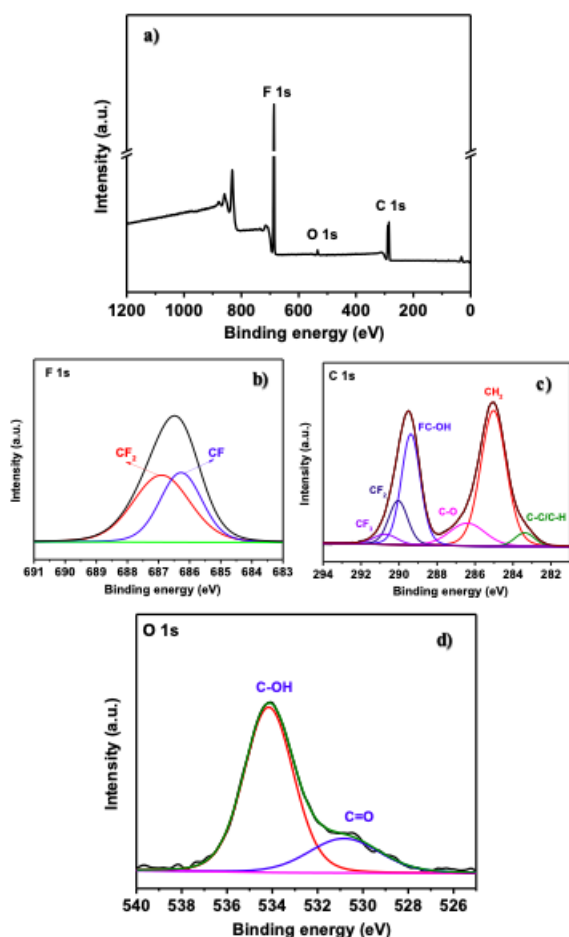


Figure 4 XPS spectra of PVDF/CTAB nanofibers: Wide XPS and high-resolution (a) F1s (b); C1s (c) and O1s spectra (d).

To the best of our knowledge, this effect has not been previously mentioned in the literature, and the explanation requires additional research. The rate constants (k) were calculated from the kinetic curves according to the pseudo-first order equation and are presented in Figure 5b:

$$\ln(C_0/C) = k t. \quad (4)$$

The k values were 0.011, 0.018, 0.021, 0.043, and 0.046 min^{-1} for sonolysis, photolysis, piezocatalysis, photocatalysis, and piezophotocatalysis, respectively. During piezocatalysis, the reaction rate increased by a factor of 1.91 compared to sonolysis, indicating the generation of the PVDF/CTAB piezopotential under ultrasonic treatment. During photocatalysis, the reaction rate increased by a factor of 2.4 compared with photolysis, indicating the photogeneration of electron-hole pairs upon irradiation with UV-visible light.

These data indicate that the as-synthesized PVDF/CTAB composite membranes have a certain photocatalytic activity, and the comparable values reported in the literature are shown in Table 1.

3.1. Mechanism

According to the classical concepts, the photocatalytic reaction can be generally divided into three stages:

(1) after the absorption of photons by a semiconductor, electron-hole pairs are formed in the volume;

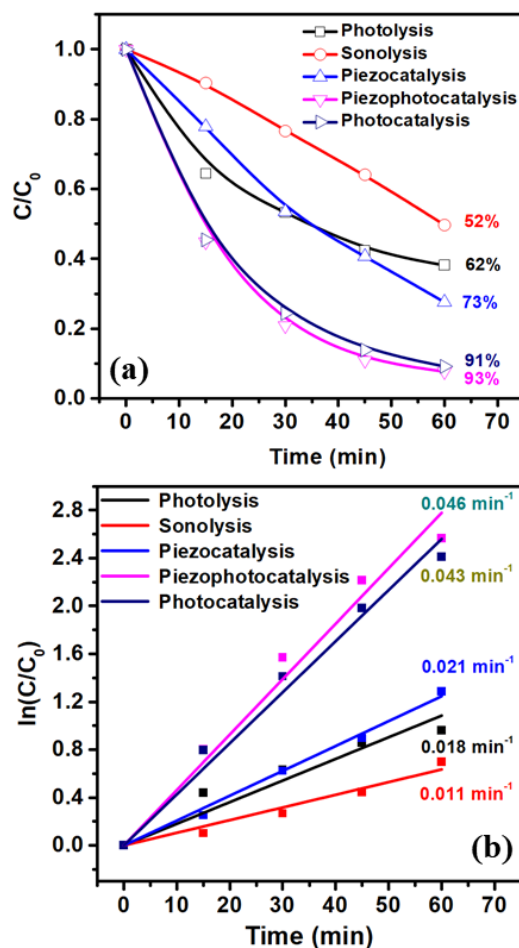


Figure 5 MB degradation curves (1 mg L^{-1} , 20 mL) (a); time dependence of $\ln(C/C_0)$ for PVDF/CTAB nanofibers (b).

(2) the photogenerated electrons and holes, meanwhile, separate and migrate to the surface of the photocatalyst;

(3) the photogenerated charge carriers participate in the redox reaction on the surface of the photocatalyst leading to the generation of reactive oxygen species.

To find out by what mechanism the photocatalytic reaction proceeds, the experiments were carried out with traps for reactive oxygen species. Generally, superoxide radicals ($\cdot\text{O}_2^-$), holes (h^+), electrons (e^-) and hydroxyl radicals ($\cdot\text{OH}$) are considered to be the potential dominant active species in the photocatalytic decomposition process. We used isopropanol (IP) for fixing hydroxyl radicals ($\cdot\text{OH}$), ethylenediaminetetraacetic acid (EDTA) for holes (h^+), benzoquinone (BZQ) for superoxide radicals ($\cdot\text{O}_2^-$) and silver nitrate (AgNO_3) for electrons (e^-) respectively. The data are presented in Figure 6.

When irradiated with light, PVDF/CTAB is excited, producing electrons and holes. The holes, migrating to the surface, enter into chemical reactions, oxidizing OH^- with the formation of $\cdot\text{OH}$. Thus, MB decomposes at the expense of h^+ and $\cdot\text{OH}$ in the reaction system.

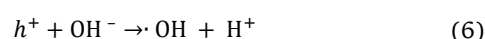
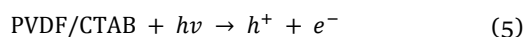


Table 1 Comparison of photocatalytic contaminant removal rates by immobilized catalyst on PVDF substrates.

Photocatalyst	Pollutant	Light source	Efficiency	Ref
PVDF/GO/ZnO	MB, 60 mL, 10 mg L ⁻¹	Xenon, 300W	86.8% (100 min)	[25]
PVDF/ZIF-8/ZnO	MB, 100 mL, 10 mg L ⁻¹	Xenon, 300W	95% (4.5 h)	[26]
PVDF/TiO ₂	RhB, 10 ppm	LED, 18 W	80% (6 h)	[27]
PVDF/TiO ₂ /g-C ₃ N ₄	RhB, 50 mL, 5 mg L ⁻¹	Xenon, 800 W	78% (180 min)	[28]
SnO ₂ /TiO ₂ /PVDF	RhB, 100 mL, 10 mg L ⁻¹	Xenon, 250W	92% (270 min)	[29]
TiO ₂ /PVDF	MB, 300 mL, 10 ppm	High-pressure mercury lamp	95% (60 min)	[30]
PVDF/GO	MB, 150 mL, 10 μmol L ⁻¹	Xenon, 150W	83% (360 min)	[31]
PVDF-GO/NB-TiO ₂	MB, 50 mL, 5 mg L ⁻¹	Halogen lamp, 500W	39% (30 min)	[32]
PVDF-B ₄ C	MB, 50 mL, 50 mg L ⁻¹	UV lamp	96% (20 min)	[33]
PVDF/ZnO/Ag ₂ O	MB, 30 mL, 10 mg L ⁻¹	UV light, 6 W	97.2% (210 min)	[34]
PVDF/CTAB	MB, 20 mL, 1 mg L ⁻¹	High-pressure mercury lamp,	91% (60 min)	This work

Since electrons have little effect on the MB degradation, they will accumulate in the conduction band. Probably, the accumulation of excess negative charge acts as an inhibitor for the piezopotential, or as a depolarizer of the piezo field. It should be noted that a clear deactivation of the catalytic activity manifests itself when IP is added to the reaction system, at which the efficiency of MB decomposition decreased from 91% to 12.0%. This indicates the dominant role of hydroxyl radicals ·OH. Holes also play an important role in the course of the reaction, because with the addition of EDTA, the decomposition efficiency was 60%. With the addition of AgNO₃ and benzoquinone, the decomposition efficiency was 86 and 82%, which indicates a small contribution of e⁻ and ·O₂⁻ to the reaction.

Based on this, the proposed mechanism of photocatalytic decomposition of MB is shown in Figure 7.

4. Conclusions

Thus, it was shown that the modification of PVDF with the cationic surfactant CTAB leads to an increase in the electroactive phase due to the ion-dipole interaction. It was also shown for the first time that the addition of CTAB promotes the photosensitivity of the wide-gap dielectric polymer PVDF (the band gap is more than 6 eV). It was demonstrated that the photocatalytic decomposition efficiency is 91% in 60 minutes. The material exhibits piezocatalytic activity – 73% in 60 minutes. The experiments on trapping active oxidizing forms established that ·OH hydroxyl radicals play the main role in the photocatalytic process.

Supplementary materials

No supplementary materials are available.

Funding

This work was supported by the Russian Science Foundation (grant no. 22-73-10091), <https://www.rscf.ru/en>.

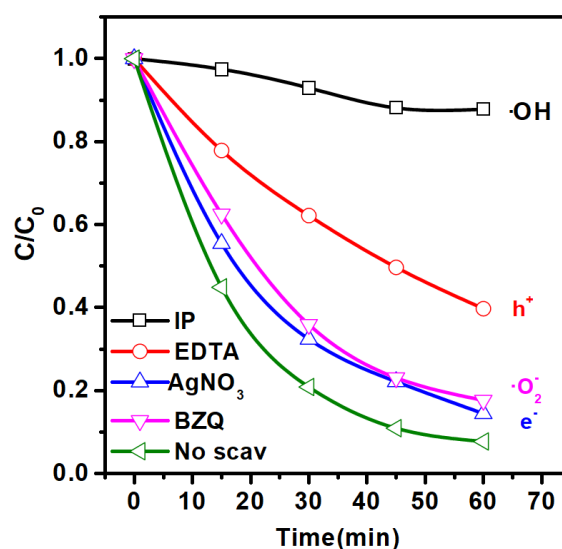


Figure 6 Photocatalytic under Uv-Vis light performance of PVDF/CTAB nanofibers for degradation of MB after adding various scavengers.

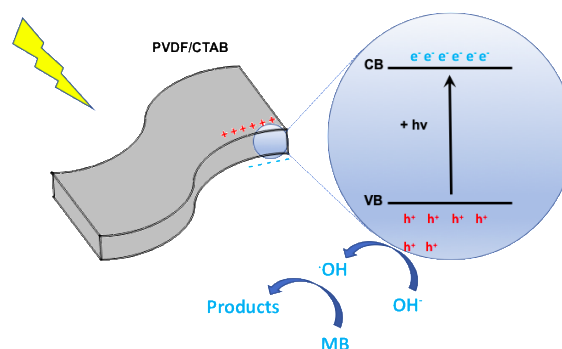


Figure 7 Schematic illustration of the photocatalytic mechanism for PVDF/CTAB.

Acknowledgments

Part of the work was carried out with the support of CEITEC Nano Research Infrastructure supported by MEYS CR (LM2018110) and the Grant Agency of the Czech Republic under project No. 19-17457S.

Author contributions

Conceptualization: F.O., D.So.
 Data curation: A.Sh., R.G.
 Formal Analysis: Sh.R., D.So., F.O.
 Funding acquisition: F.O., D.So.
 Investigation: D.Se., K.C., A.R., M.A., R.G., A.Sh.
 Methodology: D.Se., K.C., F.O.
 Project administration: F.O.
 Resources: D.So., K.C., F.O.
 Software: Sh.R.,
 Supervision: F.O.
 Validation: D.So., Sh.R.
 Visualization: D.Se.
 Writing – original draft: F.O.
 Writing – review & editing: F.O., D.So.

Conflict of interest

The authors declare no conflict of interest

Additional information

Author IDs:

Alina Rabadanova, Scopus ID [57429741000](https://orcid.org/57429741000), [Colab](https://colab.ws/labs/282)
 Magomed Abdurakhmanov, Scopus ID [57291263400](https://orcid.org/57291263400), [Colab](https://colab.ws/labs/282)
 Rashid Gulakhmedov, Scopus ID [57291948600](https://orcid.org/57291948600), [Colab](https://colab.ws/labs/282)
 Abdulatip Shuaibov, Scopus ID [57291948700](https://orcid.org/57291948700), [Colab](https://colab.ws/labs/282)
 Daud Selimov, Scopus ID [57292170300](https://orcid.org/57292170300), [Colab](https://colab.ws/labs/282)
 Dinara Sobola, Scopus ID [57189064262](https://orcid.org/57189064262)
 Klára Částková, Scopus ID [6508308746](https://orcid.org/6508308746)
 Shikgasan Ramazanov, Scopus ID [23100974400](https://orcid.org/23100974400)
 Farid Orudzhev Scopus ID [57201133063](https://orcid.org/57201133063), [Colab](https://colab.ws/labs/282)

Websites:

Dagestan State University, <https://dgu.ru>;
 Brno University of Technology, <https://www.vut.cz/en>;
 Amirkhanov Institute of Physics of Dagestan Federal Research Center, Russian Academy of Sciences, <http://www.dagphys.ru>;
 Immanuel Kant Baltic Federal University, <https://eng.kantiana.ru>.



**SMART
MATERIALS**
laboratory

<https://smart-mat.ru/>, <https://colab.ws/labs/282>, 

References

- Ma D, Yi H, Lai C, Liu X, Huo X, An Z, Yang L. Critical review of advanced oxidation processes in organic wastewater treatment. *Chemosphere*. 2021;275:130104. doi:[10.1016/j.chemosphere.2021.130104](https://doi.org/10.1016/j.chemosphere.2021.130104)
- Wang H, Li X, Zhao X, Li C, Song X, Zhang P, & Huo, P. A review on heterogeneous photocatalysis for environmental remediation: From semiconductors to modification strategies. *Chin J Catal*. 2022;43(2):178–214. doi:[10.1016/j.chemosphere.2021.130104](https://doi.org/10.1016/j.chemosphere.2021.130104)
- Wang, Zhong Lin. Piezotronic and piezophototronic effects. *J Phys Chem Lett*. 2010;1(9):1388–1393. doi:[10.1021/jz100330j](https://doi.org/10.1021/jz100330j)
- Liang Z, Yan CF, Rtimi S, Bandara J. Piezoelectric materials for catalytic/photocatalytic removal of pollutants: Recent advances and outlook. *Appl Catal Environ*. 2019;241:256–269. doi:[10.1016/j.apcatb.2018.09.028](https://doi.org/10.1016/j.apcatb.2018.09.028)
- Jamal MA, Sajid TA, Saeed M, Naseem B, Muneer M. Explication of molecular interactions between leucine and pharmaceutical active ionic liquid in an aqueous system: Volumetric and acoustic studies. *J Molec Liq*. 2022;119–510. doi:[10.1016/j.molliq.2022.119510](https://doi.org/10.1016/j.molliq.2022.119510)
- He H, Fu Y, Zang W, Wang, Q, Xing L, Zhang Y, Xue X. A flexible self-powered T-ZnO/PVDF/fabric electronic-skin with multi-functions of tactile-perception, atmosphere-detection and self-clean. *Nano Energy*. 2017;31:37–48. doi:[10.1016/j.nanoen.2016.11.020](https://doi.org/10.1016/j.nanoen.2016.11.020)
- Lin, Hung-Ming, and Kao-Shuo Chang. Synergistic piezophotocatalytic and photoelectrochemical performance of poly(vinylidene fluoride)-ZnSnO₃ and poly(methyl methacrylate)-ZnSnO₃ nanocomposites. *RSC Adv*. 2017;7(49):30513–30520. doi:[10.1039/C7RA05175A](https://doi.org/10.1039/C7RA05175A)
- Kadiev MV, Shuaibov AO, Abdurakhmanov MG, Selimov DA, Gulakhmedov RR, Rabadanova AA, Orudzhev FF. Synthesis and investigation of piezophotocatalytic properties of polyvinylidene fluoride nanofibers modified with titanium dioxide. *Moscow Univ Chem Bull*. 2022;77(5):256–261. doi:[10.3103/S0027131422050054](https://doi.org/10.3103/S0027131422050054)
- Orudzhev F, Ramazanov S, Sobola D, Kaspar P, Trčka T, Částková K, Kadiev M. Ultrasound and water flow driven piezophototronic effect in self-polarized flexible α -Fe₂O₃ containing PVDF nanofibers film for enhanced catalytic oxidation. *Nano Energy*. 2021;90:106–586. doi:[10.1016/j.nanoen.2021.106586](https://doi.org/10.1016/j.nanoen.2021.106586)
- Pisarenko T, Papež N, Sobola D, Tãlu Ș, Částková K, Škarvada P, Kaštyl J. Comprehensive characterization of PVDF nanofibers at macro- and nanolevel. *Polym*. 2022;14(3):593. doi:[10.3390/polym14030593](https://doi.org/10.3390/polym14030593)
- Surmenev RA, Chernozem RV, Pariy IO, Surmeneva MA. A review on piezo- and pyroelectric responses of flexible nano- and micropatterned polymer surfaces for biomedical sensing and energy harvesting applications. *Nano Energy*. 2021;79:105442. doi:[10.1016/j.nanoen.2020.105442](https://doi.org/10.1016/j.nanoen.2020.105442)
- Surmenev RA, Orlova T, Chernozem R.V, Ivanova A.A, Bartasyte A, Mathur S, Surmeneva MA. Hybrid lead-free polymer-based nanocomposites with improved piezoelectric response for biomedical energy-harvesting applications: A review. *Nano Energy*. 2019;62:475–506. doi:[10.1016/j.nanoen.2019.04.090](https://doi.org/10.1016/j.nanoen.2019.04.090)
- Zakria HS, Othman MHD, Kamaludin R, Kadir SHSA, Kurniawan TA, Jilani A. Immobilization techniques of a photocatalyst into and onto a polymer membrane for photocatalytic activity. *RSC advances*. 2021;11(12):6985–7014. doi:[10.1039/D0RA10964A](https://doi.org/10.1039/D0RA10964A)
- Li Y, Xu JZ, Zhu L, Xu H, Pan MW, Zhong GJ, Li ZM. Multiple stage crystallization of gamma phase poly(vinylidene fluoride) induced by ion-dipole interaction as revealed by time-resolved FTIR and two-dimensional correlation analysis. *Polym*. 2014;55(18):4765–4775. doi:[10.1016/j.polymer.2014.07.022](https://doi.org/10.1016/j.polymer.2014.07.022)
- Li Y, Xu JZ, Zhu L, Zhong GJ, Li ZM. Role of ion-dipole interactions in nucleation of gamma poly(vinylidene fluoride) in the presence of graphene oxide during melt crystallization. *J Phys Chem B*. 2012;116(51):14951–14960. doi:[10.1021/jp3087607](https://doi.org/10.1021/jp3087607)
- Song L, Sun S, Zhang S, Wei J. Hydrogen production and mechanism from water splitting by metal-free organic polymers PVDF/PVDF-HFP under drive by vibrational energy. *Fuel*. 2022;324:124572. doi:[10.1016/j.fuel.2022.124572](https://doi.org/10.1016/j.fuel.2022.124572)
- Liu X, Xu S, Kuang X, Wang X. Ultra-long MWCNTs highly oriented in electrospun PVDF/MWCNT composite nanofibers

- with enhanced β phase. RSC Adv. 2016;6:106690–106696. doi:[10.1039/C6RA24195F](https://doi.org/10.1039/C6RA24195F)
18. Castkova K, Kastyl J, Sobola D, Petrus J, Stastna E, Riha D, Tofel P. Structure–properties relationship of electrospun pvdf fibers. Nanomater. 2020;10(6):1221. doi:[10.3390/nano10061221](https://doi.org/10.3390/nano10061221)
19. Gang C, Zhang J, Yang S. Fabrication of hydrophobic fluorinated amorphous carbon thin films by an electrochemical route. Electrochem Commun. 2008;10(1):7–11. doi:[10.1016/j.elecom.2007.10.006](https://doi.org/10.1016/j.elecom.2007.10.006)
20. Sobola D, Kaspar P, Částková K, Dallaev R, Papež N, Sedlák P, Holcman V. PVDF Fibers Modification by Nitrate Salts Doping. Polym. 2021;13(15):2439. doi:[10.3390/polym13152439](https://doi.org/10.3390/polym13152439)
21. Kaspar P, Sobola D, Částková K, Dallaev R, Šťastná E, Sedlák P, Holcman V. Case study of polyvinylidene fluoride doping by carbon nanotubes. Mater. 2021;14(6):1428. doi:[10.3390/ma14061428](https://doi.org/10.3390/ma14061428)
22. Mohammadi Ghalehi M, Al Balushi A, Kaviani S, Tavakoli E, Bavarian M, Nejati S. Fabrication of Janus membranes for desalination of oil-contaminated saline water. ACS Appl Mater Interfaces. 2018;10(51):44871–44879. doi:[10.1021/acsami.8b16621](https://doi.org/10.1021/acsami.8b16621)
23. Shokr FS. The influence of dipoles orientation on the charge transport mechanism of Au/rr-P3HT/P (VDF-TrFE) heterojunction diode in the form of 1D-line grating nanostructure arrays. Res Phys. 2019;12:754–758. doi:[10.1016/j.rinp.2018.12.033](https://doi.org/10.1016/j.rinp.2018.12.033)
24. Zhu Q, Zhang K, Li D, Li N, Xu J, Bahnemann DW, Wang C. Polarization-enhanced photocatalytic activity in non-centrosymmetric materials based photocatalysis: A review. Chem Eng J. 2021;426:131681. doi:[10.1016/j.cej.2021.131681](https://doi.org/10.1016/j.cej.2021.131681)
25. Zhang D, Dai F, Zhang P, An Z, Zhao Y, Chen L. The photodegradation of methylene blue in water with PVDF/GO/ZnO composite membrane. Mater Sci Eng. 2019;96:684–692. doi:[10.1016/j.msec.2018.11.049](https://doi.org/10.1016/j.msec.2018.11.049)
26. Tang T, Li C, He W, Hong W, Zhu H, Liu G, Lei C. Preparation of MOF-derived C-ZnO/PVDF composites membrane for the degradation of methylene blue under UV-light irradiation. J Alloys Compd. 2022;894:162559. doi:[10.1016/j.jallcom.2021.162559](https://doi.org/10.1016/j.jallcom.2021.162559)
27. Lou L, Wang J, Lee YJ, Ramkumar SS. Visible light photocatalytic functional TiO₂/PVDF nanofibers for dye pollutant degradation. Particle Systems Characteriz. 2019;36(9):1900091. doi:[10.1002/ppsc.201900091](https://doi.org/10.1002/ppsc.201900091)
28. Zhou TT, Zhao FH, Cui YQ, Chen LX, Yan JS, Wang XX, Long Y.Z. Flexible TiO₂/PVDF/g-C₃N₄ nanocomposite with excellent light photocatalytic performance. Polym. 2019;12(1):55. doi:[10.3390/polym12010055](https://doi.org/10.3390/polym12010055)
29. Hong W, Li C, Tang T, Xu H, Yu Y, Liu G, Zhu H. The photocatalytic activity of the SnO₂/TiO₂/PVDF composite membrane in rhodamine B degradation. New J Chem. 2021;45(5):2631–2642. doi:[10.1039/DoNJo4764C](https://doi.org/10.1039/DoNJo4764C)
30. Dzinun H, Ichikawa Y, Mitsuhiro H, Zhang Q. Efficient immobilised TiO₂ in polyvinylidene fluoride (PVDF) membrane for photocatalytic degradation of methylene blue. Journal of Membrane Sci Res. 2020;6(2):188–195. doi:[10.1039/DoNJo4764C](https://doi.org/10.1039/DoNJo4764C)
31. Alyarnezhad S, Marino T, Parsa J.B, Galiano F, Ursino C, Garcia H, Figoli A. Polyvinylidene fluoride-graphene oxide membranes for dye removal under visible light irradiation. Polym. 2020;12(7):1509. doi:[10.3390/polym12071509](https://doi.org/10.3390/polym12071509)
32. Abdelmaksoud M, Mohamed A, Sayed A, Khairy S. Physical properties of PVDF-GO/black-TiO₂ nanofibers and its photocatalytic degradation of methylene blue and malachite green dyes. Environ Sci Pollut Res. 2021;28(24):30613–30625. doi:[10.1007/s11356-021-12618-1](https://doi.org/10.1007/s11356-021-12618-1)
33. Ouyang Y, Otitoju TA, Jiang D, Li S, Shoparwe NF, Wang S, Zhang A. Synthesis of PVDF-B4C mixed matrix membrane for ultrafiltration of protein and photocatalytic dye removal. J Appl Polym Sci. 2022;139(8):51663. doi:[10.1002/app.51663](https://doi.org/10.1002/app.51663)
34. Zang C, Han X, Chen H, Zhang H, Lei Y, Liu H, Ge M. In situ growth of ZnO/Ag₂O heterostructures on PVDF nanofibers as efficient visible-light-driven photocatalysts. Ceram Int. 2022;48(19):27379–27387. doi:[10.1016/j.ceramint.2022.05.312](https://doi.org/10.1016/j.ceramint.2022.05.312)